An Analysis of the Unbalanced Three Phase Fault in the Transmission Line

R.Mohd Ghazali[1*], W.Dominic[1], S.N.B.Zawawi[1], R.Sinnadurai[1]
[1] Faculty of Engineering and Life Sciences, Bestari Jaya Campus, Universiti Selangor, Selangor, Malaysia
[*]corresponding author's email: aiza@unisel.edu.my

Abstract – *In this paper, unbalanced three-phase fault in transmission lines is considered with respect to estimating the state of power system after a fault occurs at different buses. Faults such as a single-line-to-ground (SLG), line-to-line (LL) and double-line-to-ground (DLG) affect the bus system that is connected along with the transmission line. MATLAB software was employed in which unbalanced fault programs based on the Symmetrical Component method to determine the voltage magnitudes, line current magnitude, total fault current, real and reactive power at Phase A, Phase B and also on phase C for the different bus lines. The unbalanced fault programs are executed using a Newton Raphson based power flow program for the standard IEEE 14, IEEE 26 and IEEE 30 bus systems. The obtained results show that the single line to ground fault is the most severe kind for IEEE 14 bus system, while for IEEE 26 and IEEE 30 bus system, the most severe fault is line to line fault. This finding is crucial for evaluating the reliability and stability of power transmission lines.*

Keywords: *Newton Raphson, Power Flow, Unbalanced Three-Phase Fault*

Article History
Received 26 August 2024
Received in revised form 21 October 2024
Accepted 3 December 2024

I. Introduction

The electric power generated in the power plant will be raised in terms of voltage level with the support of the transformer before the electricity is transmitted and distributed with large, interconnected power systems. Transmission lines are essential parts of modern power networks. They serve an important role in distributing electricity, and faults in these lines can cause substantial disruptions in power supply [1]. High voltage is delivered in the transmission line to minimize transmission losses and thus be able to ensure continuous power supply in power systems without problems [2]. Faults that can happen on any transmission line are known as balanced faults and unbalanced faults. Three-phase balanced faults and unbalanced faults are two types of power system faults. Unbalanced faults on electricity transmission lines can be classified into three types: single line-to-ground, line-to-line, and double line-to-ground [3]. An unbalanced fault is known as the most common fault that happens in transmission lines [4]. Understanding how three-phase unbalance affects distribution equipment losses is essential for ensuring reliable and efficient operation of power distribution networks. Therefore, fault analysis is one of the proper ways to evaluate the fault currents and voltages in power systems. The fault analysis results are important for the power system design, the protection system setting, and power quality considerations [5]. Faults in transmission lines are caused by circuit failures that disrupt the regular flow of current. A short circuit or open circuit fault creates an undesired conducting route, preventing current flow [6]. Faults can cause major interruptions, thus rapid detection and classification is critical for effective management [7].

The symmetrical component method continues to be a crucial analytical tool for managing unbalanced faults in electrical power systems. Proper analyses of unbalanced three-phase fault systems need to be done to understand the power quality of the power system after the fault occurs.

This study will analyze the performance in term of voltage magnitude and current magnitude in each phase under unbalanced fault condition. Other than that, it focuses on obtaining the total fault current; bus voltages

line current, real and reactive power during fault by analyzing three different IEEE bus systems which are 14, 26 and 30 busses by running through MATLAB software.

II. Literature Review

Three-phase faults and unbalanced faults, in general are very challenging for power systems because of their destruction on system stability, power quality and equipment life. The symmetrical component method (SCM) is usually used to simplify the computation and detection of unbalanced faults due to its capabilities that can decouple asymmetrical fault phasors into components. C. L. Fortescue in 1918 first introduced the SCM, which is very important to simplify the analysis of unbalanced faults for power systems [8]. Fortescue's 1918 symmetrical components theory and Lyon's 1954 time-domain analysis have been widely employed in fault analysis and power system protection methods, respectively [9]. By transforming unbalanced phasors into symmetrical components, it allows engineers to establish a more organized approach to dealing with complicated fault conditions. Moreover, Fortescue's theorem, unbalanced faults can be solved by separating them into three independent symmetrical components. Each of these components will differ in the phase sequence; a positive, negative and a zero sequence as shows in Fig.1.

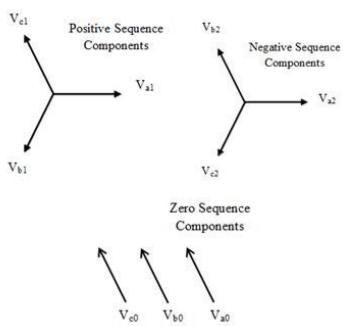

Fig. 1. Phase sequence: a positive, negative and a zero sequence

Recent studies have been carried out. According to [10], this paper presents a wide-ranging history of the symmetrical component method in terms of applications to contemporary grids and discusses its evolution regarding handling unbalanced circumstances entailed with renewable-heavy systems. Unbalanced faults include single-line-to-ground (SLG), line-to-line (LL) and double-line-to ground faults in three-phase transmission lines. These faults lead to unbalance in current and voltage which are studied because otherwise, the system may not stand. Next, [11] investigate on a comprehensive study of unbalanced faults and their impacts on the stability of transmission lines as well power quality. As stated in the paper, an accurate fault diagnosis is essential to check the cascading failures within a grid, hence ruler based on misfault is defined which help for better fault direction.

The Newton-Raphson (NR) method is applied for analyzing unbalance three-phase fault conditions as presented in [12]. This work probes the amalgamation of the algorithm by which it can be reformed to essentially determine power flow equations during faults on steady state. The authors [13] demonstrate how the NR method converges under different fault scenarios. Recent studies suggest that a combination of optimization or algorithmic model and Newton-Raphson methods in unbalanced fault programs are very promising. This technique uses the NR approach to evaluate numerical solutions for the entire network power flow and voltage profile in order to swiftly find and resolve issues.

III. Methodology

The process and procedures utilized for an unbalanced three-phase faults system are introduced. The technique can be proved via the flow chart in Fig. 2.

The algorithm will be run using MATLAB software using three test systems which are IEEE 14-bus system, IEEE 26-bus system, and IEEE 30-bus system where the result will determine the total fault current, line current, and bus voltage as well as real and reactive power.

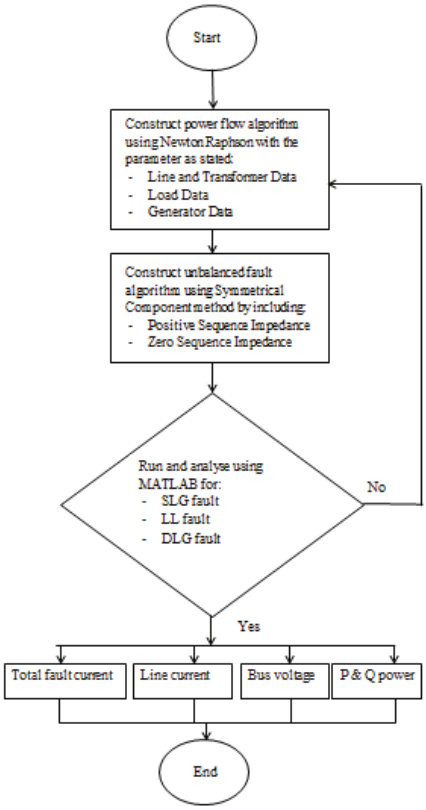

Fig. 2. Flowchart for unbalanced three phase fault program.

A. Case Study 1: IEEE 14 Bus System

Fig. 3 shows the two generators located at bus 1 and bus 2 and three compensators are at bus 3, 6, and 8. Other buses are considered as load bus for IEEE 14 bus system [14]. Base MVA for this system is 100 MVA [15].

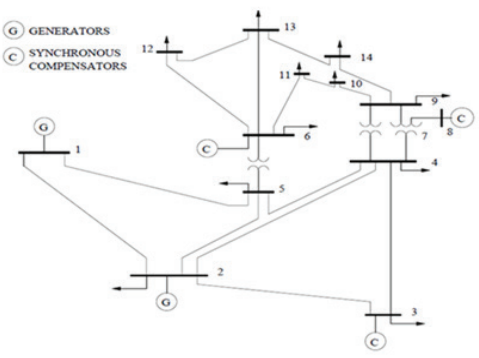

Fig. 3. IEEE 14 bus system

B. Case Study 2: IEEE 26 Bus System

Fig. 4 shows a single line diagram of the IEEE 26 bus system. Bus 1 voltage is specified as $V_1 = 1.025\angle 0°$, is taken as a slack bus. Five of the generators are connected to buses 2, 3, 4, 5, and 26. The bus that connected along transformer is bus 2, 3, 4, 6, 7, 8, 9, 12, 13 and 19. Base MVA for this system is 100 MVA [16].

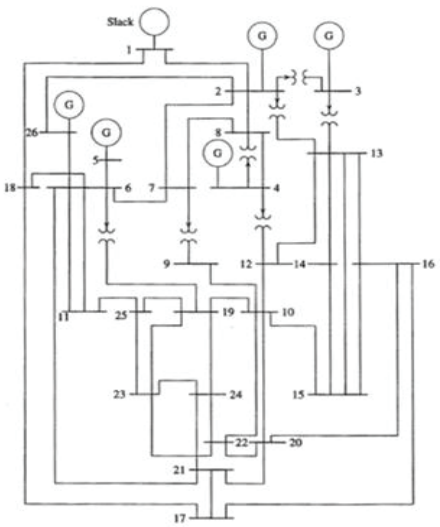

Fig. 4. IEEE 26 bus system

C. Case Study 3: IEEE 30 Bus System

Fig.5 shows a single line diagram of IEEE 30 bus system which has five generators connected to bus 2, 5, 8, 11, and 13. Bus 1 voltage is specified as $V_1 = 1.060\angle 0°$, is taken as a slack bus. Base MVA for this system is 100 MVA [17].

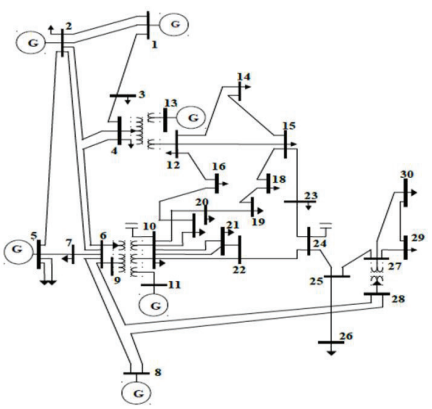

Fig. 5. IEEE 30 bus system

IV. Results and Discussions

This section presents the results from three different case studies produced by running unbalance fault analysis program to determine bus voltage, line current and total fault current and represented in per unit (p.u) corresponding to the fault at different buses by using graphical form. Symmetrical component method has been used in unbalanced fault program with positive and zero sequence impedance data to analyze SLG, LL and DLG fault. In addition, for voltage magnitude and line current include the three phases A, B, and C. The pre-fault bus voltages are specified to 1.0 per unit. Only selected bus line 2, 5, 8, 11 and 14 were identified for the Case Study 1, while bus line 2, 5, 8, 11 and 14, 17, 20, 23 and 26 were identified for the Case Study 2 and bus line 2, 5, 8, 11 and 14, 17, 20, 23, 26 and 29 were identified for the Case Study 3.

A. Case Study 1: IEEE 14 Bus system

Fig. 6 depicts the voltage magnitudes in per unit P.U. vs. bus line. According to the data, during SLG faults, Phases B and C experience higher voltages, while Phase A is grounded at 0.000 p.u. The highest voltage magnitudes in Phases B and C are at Bus 5 and Bus 14. Next, during LL faults, Phase A remains unaffected at nominal voltage 1.000 p.u, whereas Phases B and C undergo identical voltage decreases 0.5000 p.u. This result shows that the fault creates a consistent voltage decrease across the network. For the DLG faults, Phases B and C are grounded 0.000 p.u, with Phase A carrying the majority of the voltage load.

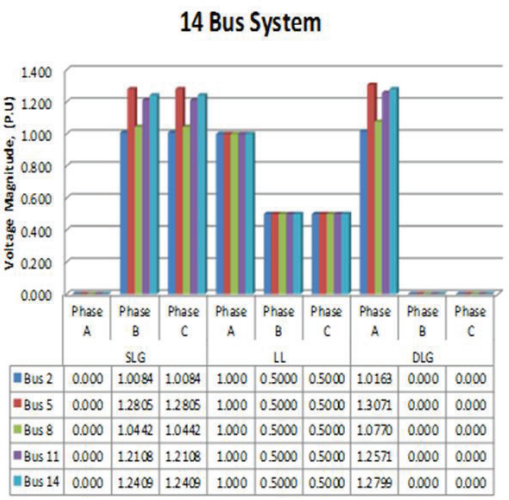

	Phase A	Phase B	Phase C	Phase A	Phase B	Phase C	Phase A	Phase B	Phase C
	SLG			LL			DLG		
Bus 2	0.000	1.0084	1.0084	1.000	0.5000	0.5000	1.0163	0.000	0.000
Bus 5	0.000	1.2805	1.2805	1.000	0.5000	0.5000	1.3071	0.000	0.000
Bus 8	0.000	1.0442	1.0442	1.000	0.5000	0.5000	1.0770	0.000	0.000
Bus 11	0.000	1.2108	1.2108	1.000	0.5000	0.5000	1.2571	0.000	0.000
Bus 14	0.000	1.2409	1.2409	1.000	0.5000	0.5000	1.2799	0.000	0.000

Fig. 6. Voltage magnitudes in per unit (P.U) vs. bus line

Fig. 7 depicts the plot of line current magnitudes in P.U. The single-phase fault SLG shows that Phase A is contributing more current for the Bus 2. The magnitude is 111.965 P.U. and the remaining buses 5, 8, 11, and 14 have current which is very less.

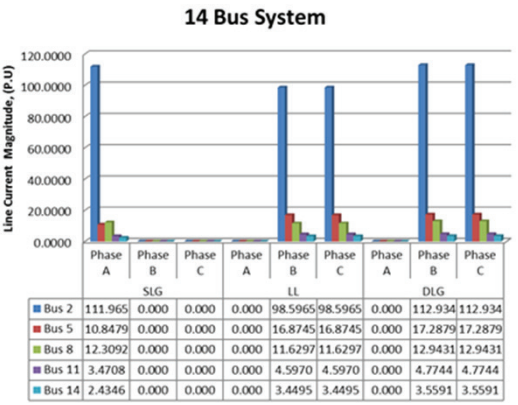

	Phase A	Phase B	Phase C	Phase A	Phase B	Phase C	Phase A	Phase B	Phase C
	SLG			LL			DLG		
Bus 2	111.965	0.000	0.000	0.000	98.5965	98.5965	0.000	112.934	112.934
Bus 5	10.8479	0.000	0.000	0.000	16.8745	16.8745	0.000	17.2879	17.2879
Bus 8	12.3092	0.000	0.000	0.000	11.6297	11.6297	0.000	12.9431	12.9431
Bus 11	3.4708	0.000	0.000	0.000	4.5970	4.5970	0.000	4.7744	4.7744
Bus 14	2.4346	0.000	0.000	0.000	3.4495	3.4495	0.000	3.5591	3.5591

Fig. 7. Line current magnitudes in per unit (P.U) vs. bus line

Next is LL in which the contribution of current is equal to Phase B and Phase C and there is no current in Phase A for all types of buses. In Phase B and C results, the Bus 2 has a higher magnitude 98.5965 p.u compared to other busses. Likewise, for DLG situation. Phases B and C have shown current, but again there is no current in phase A. In Phase B and C results, Bus 2 again has higher magnitudes compared to other busses. The pattern in phase follows the same line LL but the magnitude is higher in the DLG.

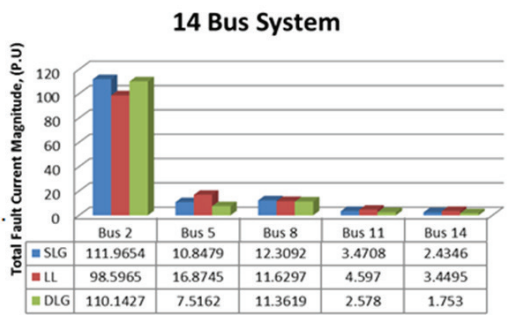

	Bus 2	Bus 5	Bus 8	Bus 11	Bus 14
SLG	111.9654	10.8479	12.3092	3.4708	2.4346
LL	98.5965	16.8745	11.6297	4.597	3.4495
DLG	110.1427	7.5162	11.3619	2.578	1.753

Fig. 8 Total fault current magnitude vs. bus line

Fig. 8 shows a graph of the fault current. Bus 2 has the largest fault current magnitude of any fault type, whereas Bus 14 has the lowest. Bus 2 exhibits very high fault current magnitudes for all fault types, particularly SLG 111.96 p.u and DLG 110.14 p.u, with LL slightly

lower but still significant at 98.59 p.u. The closeness of SLG and DLG fault levels indicates that grounding difficulties are critical at Bus 2. Bus 5 has far lower fault current magnitudes than Bus 2. LL faults create the most current (16.87 p.u), whereas DLG produces the least (7.52 p.u).

Bus 8 has a more balanced fault profile, with fault currents that are roughly equal across SLG 12.30 p.u, LL 11.63 p.u, and DLG 11.36 p.u. Bus 11 has low fault current magnitudes throughout the board, with LL being somewhat more significant (4.59 p.u). Bus 14 has the lowest fault current magnitudes of all of the bus lines, with LL 3.45 p.u being the highest and DLG 1.75 p.u the lowest. The low current levels indicate less fault exposure; however LL faults may demand more attention because they generate the highest current.

As shown in Table I, Bus 2 has a significant amount of both real and reactive load 21.7 MW and 12.70 MW, but also generates more power than it consumes, contributing both real and reactive power to the system also contributing to the system's overall power supply and voltage support. Bus 5 only consumes power, with a moderate load of real power and a smaller reactive power demand 7.60 MW and 1.60 MW. There is no generation at this bus. Bus 8 does not have any load but provides reactive power generation. This indicates that Bus 8 is primarily supporting voltage stability in the network by supplying reactive power. Bus 11 consumes a small amount of both real and reactive power 3.5 MW and 1.80 MW. There is no generation at this bus. Bus 14 is a load bus with a moderately high consumption of real and reactive power 14.9 MW and 5.000 MW. There is no generation at this bus. Bus 5, Bus 11, and Bus 14 shows they depend on other buses for their real and reactive power needs.

TABLE I
REAL AND REACTIVE POWER FOR IEEE 14 BUS SYSTEMS

BUS	LOAD		GENERATION	
LINE	P,(MW)	Q,(MVAR)	P,(MW)	Q,(MVAR)
2	21.700	12.700	40.000	46.450
5	7.600	1.600	0.000	0.000
8	0.000	0.000	0.000	20.730
11	3.500	1.800	0.000	0.000
14	14.900	5.000	0.000	0.000

B. Case Study 2: IEEE 26 Bus System

Fig. 9 shows the tabulated data for voltage magnitude. In SLG fault, Phase A are the faulted phase, which is why the voltage magnitude for Phase A is zero for all buses.

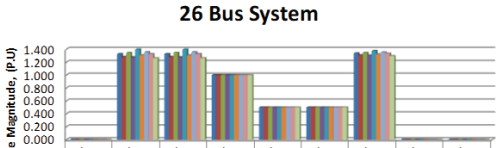

	Phase A	Phase B	Phase C	Phase A	Phase B	Phase C	Phase A	Phase B	Phase C
	SLG			LL			DLG		
Bus 2	0.000	1.3275	1.3275	1.000	0.5000	0.5000	1.3360	0.000	0.000
Bus 5	0.000	1.2811	1.2811	1.000	0.5000	0.5000	1.3075	0.000	0.000
Bus 8	0.000	1.3443	1.3443	1.000	0.5000	0.5000	1.3456	0.000	0.000
Bus 11	0.000	1.278	1.278	1.000	0.5000	0.5000	1.3055	0.000	0.000
Bus 14	0.000	1.3972	1.3972	1.000	0.5000	0.5000	1.3736	0.000	0.000
Bus 17	0.000	1.3058	1.3058	1.000	0.5000	0.5000	1.3231	0.000	0.000
Bus 20	0.000	1.3547	1.3547	1.000	0.5000	0.5000	1.3514	0.000	0.000
Bus 23	0.000	1.3267	1.3267	1.000	0.5000	0.5000	1.3356	0.000	0.000
Bus 26	0.000	1.2636	1.2636	1.000	0.5000	0.5000	1.2959	0.000	0.000

Fig. 9 Voltage magnitudes in per unit (P.U) vs. bus line

The voltage collapses because this phase is directly involved in the fault. Bus 2, Bus 5, Bus 8, Bus 11, Bus 14 and so on has 0.000 p.u in Phase A which indicate that the system is unbalanced due to the fault in this phase. For Phase B and Phase C, the voltage magnitudes remain relatively high. For each bus, the voltages are close to the nominal voltage value of 1.3 p.u for all buses though slight variations occur. This indicates that although the system is unbalanced, Phases B and C are still supplying voltage close to the nominal level. Likewise, for LL fault, for Phase A the voltage remains at 1.000 p.u for all buses, which represents the nominal voltage. The LL fault only involves Phases B and C, leaving Phase A unaffected. The uniform voltage across all buses in Phase A. Phases B and C the voltage magnitudes are reduced to 0.5000 p.u. across all buses. This reduction is a direct consequence of the fault involving these two phases. The drop to half the nominal voltage indicates that these phases are under fault stress, leading to voltage imbalance. Every bus for example Bus 2, Bus 5, Bus 8, and so on shows the same magnitude for these phases during the fault, confirming the unbalanced nature of the system in this condition. Meanwhile, during the DLG fault, Phase A stays unaffected and has a higher voltage magnitude than the SLG and LL faults. Bus 14 has a voltage of 1.3736 p.u, and Bus 2 has 1.3360 p.u. Both Phases B and C have voltages of 0.000 P.U. for all buses since they are directly involved in this issue. The voltage falls fully in these phases due to the DLG fault, which causes two of the three phases to lose voltage entirely.

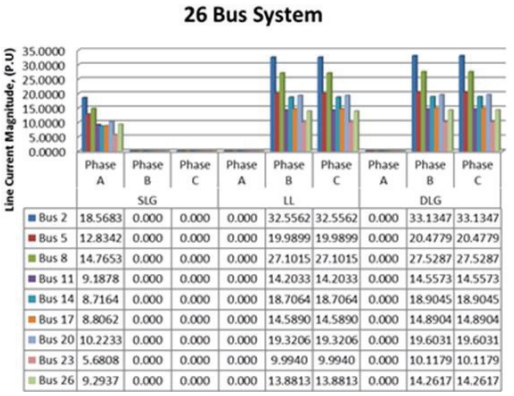

	Phase A	Phase B	Phase C	Phase A	Phase B	Phase C	Phase A	Phase B	Phase C
	SLG			LL			DLG		
Bus 2	18.5683	0.000	0.000	0.000	32.5562	32.5562	0.000	33.1347	33.1347
Bus 5	12.8342	0.000	0.000	0.000	19.9899	19.9899	0.000	20.4779	20.4779
Bus 8	14.7653	0.000	0.000	0.000	27.1015	27.1015	0.000	27.5287	27.5287
Bus 11	9.1878	0.000	0.000	0.000	14.2033	14.2033	0.000	14.5573	14.5573
Bus 14	8.7164	0.000	0.000	0.000	18.7064	18.7064	0.000	18.9045	18.9045
Bus 17	8.8062	0.000	0.000	0.000	14.5890	14.5890	0.000	14.8904	14.8904
Bus 20	10.2233	0.000	0.000	0.000	19.3206	19.3206	0.000	19.6031	19.6031
Bus 23	5.6808	0.000	0.000	0.000	9.9940	9.9940	0.000	10.1179	10.1179
Bus 26	9.2937	0.000	0.000	0.000	13.8813	13.8813	0.000	14.2617	14.2617

Fig. 10 Line Current Magnitude in per unit (P.U) vs. bus line

Fig. 10 shows the line current magnitudes vs. the bus line. Current is only present in Phase A, with no current in Phases B or C affected for all busses by the SLG fault. Bus 2 having the highest current at 18.5683 p.u followed among other busses. Meanwhile for LL Fault, there is current flow in Phases B and C, but no current in Phase A. The current magnitudes are nearly the same in both phases B and C for each bus, such as Bus 2 showing 32.5562 p.u in Phase B and 32.5562 p.u in Phase C. Buses like Bus 5 and Bus 8 exhibit significant current in this fault type. For DLG Fault, In this case, currents are observed in both Phases B and C, but none in Phase A. Similar to the LL fault, the magnitude is identical in Phases B and C for each bus, such as Bus 2 showing 33.1347 p.u. in both B and C. Bus 8, Bus 5, and Bus 14 have considerable current magnitudes during this fault type.

The graph shows in Fig.11. demonstrates the total fault current magnitudes in per unit P.U. Bus 2 experiences the highest fault current during an LL fault, and a moderate current during SLG and DLG faults. During the LL fault, Bus 2, Bus 5 also sees the highest current followed by SLG and DLG faults. Bus 8 follows a similar pattern, with LL faults causing the largest fault currents, while DLG fault currents are the smallest. Bus 11 also sees the highest current during LL faults and the lowest during DLG faults. For Bus 14 the trend continues here, with LL faults producing the highest fault currents. Meanwhile for bus 17 LL faults have the highest fault current magnitudes, followed by SLG and DLG.

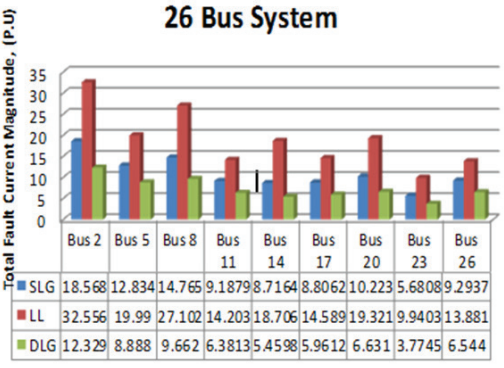

	Bus 2	Bus 5	Bus 8	Bus 11	Bus 14	Bus 17	Bus 20	Bus 23	Bus 26
SLG	18.568	12.834	14.765	9.1879	8.7164	8.8062	10.223	5.6808	9.2937
LL	32.556	19.99	27.102	14.203	18.706	14.589	19.321	9.9403	13.881
DLG	12.329	8.888	9.662	6.3813	5.4598	5.9612	6.631	3.7745	6.544

Fig. 11 Total fault current magnitude vs. bus line

Result from power flow program using Newton Raphson method is tabulated in Table II. Through the power flow program total real and reactive power for load and generation is calculated. The total real and reactive power for load is 1263.000 MW and 637.000 Mvar. The total real and reactive power for generation is 1278.541 MW and 645.354 Mvar. The maximum power mismatch for this bus system is 3.51088 x 10^{-10}.

TABLE II
REAL AND REACTIVE POWER FOR IEEE 26 BUS SYSTEM

Bus	Load		Generation	
Line	P,(MW)	Q,(Mvar)	P,(MW)	Q,(Mvar)
2	21.700	12.700	40.000	46.450
5	7.600	1.600	0.000	0.000
8	0.000	0.000	0.000	20.730
11	3.500	1.800	0.000	0.000
14	14.900	5.000	0.000	0.000
17	78.000	38.000	0.000	0.000
20	48.000	27.000	0.000	0.000
23	25.000	12.000	0.000	0.000
26	40.000	20.000	60.000	33.842

C. Case Study 3: IEEE 30 Bus System

Based on Fig. 12, result from SLG Fault shows that Phase A voltage drops to 0.000 p.u. in all buses during the SLG fault, indicating that this phase is grounded. For example, Bus 29 has the greatest voltage of 1.4179 p.u. in Phases B and C, whereas Bus 5 has 1.2560 p.u. in both phases. For LL Fault findings, the Phase A voltage remains constant at 1.0000 p.u for all busses. Phases B and C show a voltage drop of 0.5000 p.u. Other than that, for DLG Fault, Phase A voltage range between 1.29 and 1.38 p.u. across buses which Phase A is unaffected. Phases B and C have a voltage drop to 0.000 p.u across all buses, suggesting that they are grounded during the DLG fault.

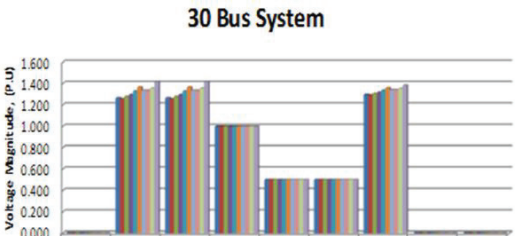

	Phase A	Phase B	Phase C	Phase A	Phase B	Phase C	Phase A	Phase B	Phase C
	SLG			LL			DLG		
Bus 2	0.000	1.26430	1.26430	1.000	0.5000	0.5000	1.29630	0.000	0.000
Bus 5	0.000	1.25600	1.25600	1.000	0.5000	0.5000	1.29060	0.000	0.000
Bus 8	0.000	1.27780	1.27780	1.000	0.5000	0.5000	1.30540	0.000	0.000
Bus 11	0.000	1.29510	1.29510	1.000	0.5000	0.5000	1.31640	0.000	0.000
Bus 14	0.000	1.32810	1.32810	1.000	0.5000	0.5000	1.33640	0.000	0.000
Bus 17	0.000	1.36420	1.36420	1.000	0.5000	0.5000	1.35650	0.000	0.000
Bus 20	0.000	1.33570	1.33570	1.000	0.5000	0.5000	1.34080	0.000	0.000
Bus 23	0.000	1.33530	1.33530	1.000	0.5000	0.5000	1.34050	0.000	0.000
Bus 26	0.000	1.35400	1.35400	1.000	0.5000	0.5000	1.35100	0.000	0.000
Bus 29	0.000	1.41790	1.41790	1.000	0.5000	0.5000	1.38380	0.000	0.000

Fig. 12 Total fault current magnitude vs. bus line

Graph in Fig. 13 depicts the line current magnitudes per unit, p.u, vs bus line. Phase A is the only phase where current flows, whereas Phases B and C show zero current for all buses.

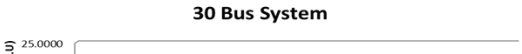

	Phase A	Phase B	Phase C	Phase A	Phase B	Phase C	Phase A	Phase B	Phase C
	SLG			LL			DLG		
Bus 2	13.3439	0.000	0.000	0.000	19.9627	19.9627	0.000	20.507	20.507
Bus 5	9.5617	0.000	0.000	0.000	14.0276	14.0276	0.000	14.432	14.432
Bus 8	8.9869	0.000	0.000	0.000	13.8882	13.8882	0.000	14.235	14.235
Bus 11	4.7905	0.000	0.000	0.000	7.7249	7.7249	0.000	7.897	7.897
Bus 14	2.0770	0.000	0.000	0.000	3.6474	3.6474	0.000	3.712	3.712
Bus 17	2.4925	0.000	0.000	0.000	4.8411	4.8411	0.000	4.907	4.907
Bus 20	1.9434	0.000	0.000	0.000	3.4837	3.4837	0.000	3.542	3.542
Bus 23	1.8712	0.000	0.000	0.000	3.3505	3.3505	0.000	3.407	3.407
Bus 26	0.6440	0.000	0.000	0.000	1.2148	1.2148	0.000	1.233	1.233
Bus 29	0.6216	0.000	0.000	0.000	1.4269	1.4269	0.000	1.440	1.440

Fig. 13 Line Current Magnitude in per unit (P.U) vs. bus line

Bus 2 has the highest current magnitude (13.3439), followed by Bus 5 (9.5617) and Bus 8 (8.9869). Lower current magnitudes are observed in Bus 29 (0.6216 P.U.) and Bus 26 (0.6440 P.U.) during SLG. Meanwhile, for the LL Fault, current flows in Phases B and C, whereas Phase A shows zero current for all buses. Bus 2 once again has the highest current, 19.9627 P.U. in both Phases B and C. During LL fault, the highest current flows at Bus 5 at 14.0276 P.U. and Bus 8 at 13.8882 P.U. For DLG Fault the results is similar to the LL fault, current is observed in Phases B and C, but there is no current in Phase A. Bus 2 has the highest current at 20.507 P.U. in both Phases B and C. Bus 5, Bus 8, and Bus 11 shows significant current magnitudes during the DLG fault and Bus 26 and Bus 29 show the lowest current magnitudes.

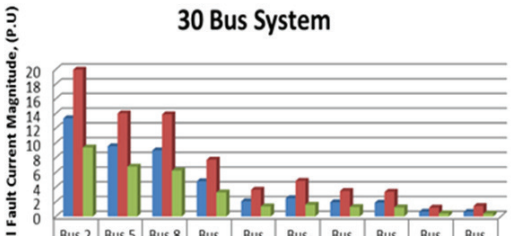

	Bus 2	Bus 5	Bus 8	Bus 11	Bus 14	Bus 17	Bus 20	Bus 23	Bus 26	Bus 29
SLG	13.344	9.5617	8.9869	4.7905	2.077	2.4925	1.9434	1.8712	0.644	0.6216
LL	19.963	14.028	13.888	7.7249	3.6474	4.8411	3.4837	3.3505	1.2148	1.4269
DLG	9.3898	6.7829	6.2426	3.2746	1.3784	1.6038	1.2812	1.234	0.418	0.383

Fig. 14 Total fault current magnitude vs bus line

Fig.14 depicts that the results for SLG Fault where highest fault current magnitude is observed at Bus 2 with 13.344 p.u. and Bus 5 with 9.5617 p.u. Baes on the observation, this fault type seems to have a significant impact on buses near the source or at critical nodes like Bus 2, Bus 5, and Bus 8, which could be due to their electrical proximity to generation sources. Buses such as Bus 29 and Bus 26 have much lower SLG fault currents 0.6216 and 0.644 p.u., suggesting less vulnerability to ground faults. Next for LL Fault result shows the highest fault current is seen at Bus 2 with 19.963 p.u. and Bus 5 with 14.028 p.u. Bus 29 and Bus 26 again show very low fault current magnitudes for LL faults. Meanwhile, the DLG fault, which is alike to SLG and LL, has the highest current at Bus 2 (9.3898 p.u.), Bus 5 (6.7829 p.u.), and Bus 8 (6.2426 p.u). Bus 2 and Bus 5 generally lowest current. Bus 29 and Bus 26 again have the lowest DLG fault current magnitudes, reinforcing their consistent behavior across fault types.

Table III shows the results of a power flow program that uses the Newton Raphson method. Moreover, through the power flow program, total real and reactive power for load and generation is calculated. The total real and reactive power for load is 283.400 MW and 126.200 Mvar. The total real and reactive power for generation is 300.928 MW and 147.121 Mvar. The maximum power mismatch for this bus system is 6.80499×10^{-9}.

TABLE III
REAL AND REACTIVE POWER FOR IEEE 30 BUS SYSTEM

Bus	Load		Generation	
Line	P_i(MW)	Q_i(Mvar)	P_i(MW)	Q_i(Mvar)
2	21.700	12.700	40.000	47.766
5	94.200	19.000	0.000	35.965
8	30.000	30.000	0.000	30.691
11	0.000	0.000	0.000	16.270
14	6.200	1.600	0.000	0.000
17	9.000	5.800	0.000	0.000
20	2.200	0.700	0.000	0.000
23	3.200	1.600	0.000	0.000
26	3.500	2.300	0.000	0.000
29	2.400	0.900	0.000	0.000

V. Conclusion and Recommendations

Analyses of unbalanced faults have been analysed and as a result various objectives are achieved by comparing results obtained on IEEE 14, 26 &30 bus systems.The result shows that after fault occur, voltage magnitude reduced to zero and fault current increase significantly at the affected phase for different unbalanced fault.

As been observed, the most severe type of unbalanced fault for IEEE 14 bus system is the single line to ground (SLG) fault, at bus line 2 with the highest total fault current magnitude. For IEEE 26 bus system, a severe type of unbalanced fault is line to line (LL) fault with the highest total fault current magnitude which is at bus line 2. For IEEE 30 bus system, a severe type of unbalanced fault is line to line (LL) fault with the highest total fault current magnitude which is at bus line 2 also. Through the power flow program, IEEE 26 bus system has the highest total real and reactive power magnitude in terms of load and generation compared to other bus systems. In recommendation, integrating SCM and NR approaches with machine learning algorithms to improve the speed and accuracy of unbalanced fault detection [18]. Furthermore, because renewable energy sources generate nonlinear and variable power inputs, standard fault detection algorithms must be improved. SCM and NR should be updated to accommodate the variability of renewable energy and inverter-dominated systems. Incorporating dynamic fault modelling techniques specific to renewables will improve transmission network fault-handling capabilities [19]. Combining the strengths of SCM and NR approaches to create hybrid fault programs might improve fault analysis, particularly in big interconnected power grids. By improving the fault analysis in interconnected power system the SCM and NR approaches to create hybrid fault programs. The on-going development of hybrid techniques will ensure that power systems can resist increasingly complicated fault circumstances [20]. Finally, to meet the needs of modern grids, fault management programs should be incorporated with real-time monitoring systems that give continuous system health updates. During system fault, real-time data analytics solutions can assist SCM and NR systems by providing operators with quick insights [21]. Overall, future fault programs can remain a viable option for boosting accuracy and adaptability in power grids.

Conflict of Interest

The authors have no conflict of interest in the publication process of the research article.

Authors Contribution

Author 1: Conceptualization, supervision and draft preparation, Author 2: Idea formulation, simulation and analysis, Author 3 and 4: Review and editorial work.

References

[1] G. Shingade and S. Shah, "Fault Detection and Location Based SVM for Three Phase Transmission Lines Applying Positive Sequence Fault Components," Trans disciplinary Journal of Engineering & Science, vol. 14, Sep. 2023, doi: 10.22545/2023/00234.

[2] J. Smith and A. Johnson, "Impact of Voltage Level on Transmission Efficiency in Power Systems," IEEE Trans. Power Syst., vol. 35, no. 4, pp. 1234-1240, Oct. 2020.

[3] K. R. Ahmed *et al.*, "Enhancing Power Grid Resilience: Advanced Strategies for Detecting and Analyzing Faults in Three-Phase Transmission Lines," vol. 31, pp. 1–5, Jun. 2024, doi: https://doi.org/10.1109/iciteics61368.2024.10625140.

[4] J. Santamaría, "Analysis of power systems under fault conditions," 2017. https://api.semanticscholar.org/CorpusID:106497028 (accessed Oct. 16, 2024).

[5] R. Brown and L. Green, "A Review of Unbalanced Faults in Transmission Lines," IEEE Access, vol. 8, pp. 567-578, 2021.

[6] A.O. Salau, J. Nweke, U. Ogbuefi, "Effective Implementation of Mitigation Measures against Voltage Collapse in Distribution Power Systems," Przegląd Elektrotechniczny, pp. 65-68, 2021. DOI: 10.15199/48.2021.10.13

[7] S. Chatterjee and N. Haque, "Fault Analysis in Three Phase Long Transmission Lines using Wavelet Transform," vol. 4, pp. 1–6, Jun. 2024, doi: https://doi.org/10.1109/apci61480.2024.10616733

[8] C. L. Fortescue, "Method of symmetrical co-ordinates applied to the solution of polyphase networks," *Proceedings of the American Institute of Electrical Engineers*, vol. 37, no. 6, pp. 629–716, Jun. 1918, doi: https://doi.org/10.1109/paiee.1918.6594104

[9] J. R. Carvajal, G. Ramos and D. F. C. Rodríguez, "Directional Relay Based on Time-Domain Symmetrical Components With Incremental Quantities," in IEEE Transactions on Industry Applications, vol. 57, no. 5, pp. 4587-4594, Sept.-Oct. 2021, doi: 10.1109/TIA.2021.3095249.

[10] K. C. Budhathoki and P. L. Shrestha, "An Overview of Symmetrical Components in Fault Analysis and Applications to Modern Power Grids," *IEEE Trans. Power Syst.*, vol. 35, no. 5, pp. 4002-4011, Sept. 2020. doi: 10.1109/TPWRS.2020.3001125.

[11] D. Sharma and R. Ghosh, "Analysis of Unbalanced Faults in Electrical Transmission Systems: A Comprehensive Review," *IEEE*

Trans. Power Deliv., vol. 36, no. 4, pp. 1501-1510, Aug. 2021. doi: 10.1109/TPWRD.2021.3075983.

[12] M. Iqbal, J. Liu, and L. Luo, "Newton-Raphson Based Power Flow Analysis for Unbalanced Three-Phase Systems Considering Fault Conditions," *IEEE Trans. Power Syst.*, vol. 36, no. 6, pp. 5230-5239, Nov. 2021. doi: 10.1109/TPWRS.2021.3080324.

[13] H. Cheng, G. Li, and M. Xu, "Enhanced Fault Location Techniques in Transmission Networks Using Symmetrical Components and Newton-Raphson Method," *IEEE Trans. Power Deliv.*, vol. 37, no. 2, pp. 2103-2112, Mar. 2023. doi: 10.1109/TPWRD.2023.3154678.

[14] S. Mahapatra and M. Singh, "Analysis of Symmetrical Fault in IEEE 14 Bus System for Enhancing Over Current Protection Scheme," *Int. J. Futur. Gener. Commun. Netw.*, vol. 9, no. 4, pp. 51–62, 2016

[15] "Load Flow Studies of IEEE-14 Bus System Using Matlab," *Int. J. Innov. Res. Dev.*, vol. 3, no. 5, pp. 149–155, 2014.

[16] H. Saadat, *Power System Analysis*, *Third Edition*: PSA Publishing LLC, ISBN: 978-0-0984543861, 2018

[17] J. ZHU, *Analysis of Transmission System Faults In The Phase Domain*, no. August. 2004

[18] M. Y. Zhang, S. R. Khan, and N. Khadem, "AI-Enhanced Fault Detection Programs for Unbalanced Systems Using Symmetrical Components and Newton-Raphson," *IEEE Trans. Ind. Electron.*, vol. 68, no. 12, pp. 12345-12355, Dec. 2022. doi: 10.1109/TIE.2022.3187564.

[19] H. Cheng, G. Li, and M. Xu, "Dynamic Simulation of Unbalanced Faults in Renewable-Integrated Power Systems Using Symmetrical Components," *IEEE Trans. Power Deliv.*, vol. 37, no. 1, pp. 1012-1021, Jan. 2023. doi: 10.1109/TPWRD.2022.3169087.

[20] H. Cheng, G. Li, and M. Xu, "Enhanced Fault Location Techniques in Transmission Networks Using Symmetrical Components and Newton-Raphson Method," *IEEE Trans. Power Deliv.*, vol. 37, no. 2, pp. 2103-2112, Mar. 2023. doi: 10.1109/TPWRD.2023.3154678.

[21] J. Zhang, M. S. Alkaabi, and K. Qian, "Challenges and Opportunities in Implementing Symmetrical Component and Newton-Raphson Methods for Fault Analysis in Renewable-Heavy Grids," *IEEE Access*, vol. 9, pp. 55674-55683, 2022. doi: 10.1109/ACCESS.2022.3174559.